International Journal for Innovative Engineering and Management Research
A Peer Revieved Open Access International Journal
www.ijiemr.org

COPY RIGHT

IJIEMR Transactions, online available on 6th July 2017. Link :
http://www.ijiemr.org/downloads.php?vol=Volume-6&issue=ISSUE-5

Title: Integration of Bidirectional Inverter By Using CUK Converter.

Volume 06, Issue 05, Page No: 1567-1578.

Paper Authors

***B.SIVA PRASANTH, I.SOBHA RANI.**

* Dept of EEE, VVIT Engineering College.

International Journal for Innovative Engineering and Management Research
A Peer Revieved Open Access International Journal
www.ijiemr.org

INTEGRATION OF BIDIRECTIONAL INVERTER BY USING CUK CONVERTER

***B.SIVA PRASANTH, **I.SOBHA RANI.**

*PG Scholar, Dept of EEE, VVIT Engineering College, Namburu; Guntur (Dt); A.P, India.

**Assistant Professor, Dept of EEE, VVIT Engineering College, Namburu; Guntur (Dt); A.P, India

ABSTRACT:

In this paper, analysis and implementation of a single phase inverter based on Cuk converter for PV system is presented. The buck-boost characteristic of such a converter promotes flexibility for both grid tied as well as standalone connections where the ac voltage is either higher than or lesser than the dc input voltage. Further Cuk based topologies have the better efficiency and voltage regulation, which is a lacking feature in a basic boost or a buck configuration. The proposed system not only offers continuous input and output current but also controlled voltage over a wider range. Hence this topology can serve as an expedient alternative converter stage for photovoltaic applications. In the proposed bidirectional two-switch Cuk converter, a controller is used for controlling the duty ratio of switching pulses. Also, this controller generates PWM signals for the switches of single phase H-bridge inverter. The Matlab/Simulink results of a Cuk converter based single phase inverter are presented. The developed scheme can easily be scalable to a much larger rating of the PV system.

Key Words: Bi-directional inverter, buck/boost MPPTs, Cuk Converter, dc-distribution applications.

I. INTRODUCTION

Renewable energy is currently widely used. One of these resources is solar energy. Photovoltaic (PV) energy is currently considered to be one of the most useful natural energy sources because it is free, abundant, pollution free, and distributed throughout the Earth. The photovoltaic (PV) array normally uses a maximum power point tracking (MPPT) technique to continuously deliver the highest power to the load when there are variations in irradiation and temperature. The disadvantage of PV energy is that the PV output power depends on weather conditions and cell temperature, making it an uncontrollable source [1]. Furthermore, it is not available during the night. However, the present energy-conversion efficiency of the PV array is still low. Therefore, in order to achieve maximum utilization efficiency, the maximum power point tracking (MPPT) control technique, which extracts the maximum possible power from the PV array, is essential in systems powered by the PV array. The PV array exhibits an extremely nonlinear voltage – ampere characteristic, which varies with array temperature and solar insulation at all times. It makes locating the maximum power point complex. Many materials can be used to manufacture solar cells, but polycrystalline Si and mono-crystalline Si are the most widely used. A thin-film solar cell can generate power under conditions of low irradiation. Therefore, the thin film solar cell has the potential to generate electrical power for a longer time than a crystalline Si solar cell. Since the thin-film cell can be easily combined with glass, plastic, and metal, it can be incorporated in green architecture. The use of thin-film solar cells has

International Journal for Innovative Engineering and Management Research
A Peer Revieved Open Access International Journal
www.ijiemr.org

increased steadily and this trend is set to continue in the future. DC-DC converter operates with MPPT algorithm to maximize power generation. DC-DC converter transfers photovoltaic energy to DC-link capacitor and increase DC-link voltage. DC-AC inverter controls DC-link voltage to certain level and transfer DC-link energy built up by DC-DC converter to grid.

And DC-AC inverter has unity power factor control to increase power transfer efficiency. If there is a good irradiance condition, the photovoltaic system can generate maximum power efficiently while an effective MPPT algorithm is used with the system. A lot of MPPT algorithms have been developed by researchers and industry delegates all over the world. They are voltage feedback method, perturbation and observation method, linear approximation method, incremental conductance method, hill climbing method, actual measurement method, and fuzzy control method and so on.

Bidirectional inverter will function as both inverter and rectifier charger mode. Bidirectional inverter is required to control the power flow between dc bus and ac grid, and to regulate the dc bus to a certain range of voltages. In the inverter mode, it converts the DC from the battery into AC electricity to supply to AC appliances. When it automatically detects availability of AC supply from the generator or the electricity grid, it will change mode into rectifier charger to charge the battery. The inverter controlled the operation by microcontroller. The significances of this needed. Bidirectional inverter are to supply pure sine wave voltage with low harmonic distortion and suitable for solar power system where AC power output is required.

In this paper design of Cuk converter controlled by MPPT technique is proposed to extract maximum power from the PV array for isolated electrical loads. The proposed system configuration and modeling is introduced. The designed system parameters are illustrated. A proposed three system configurations are introduced and simulation results are illustrated and discussed.

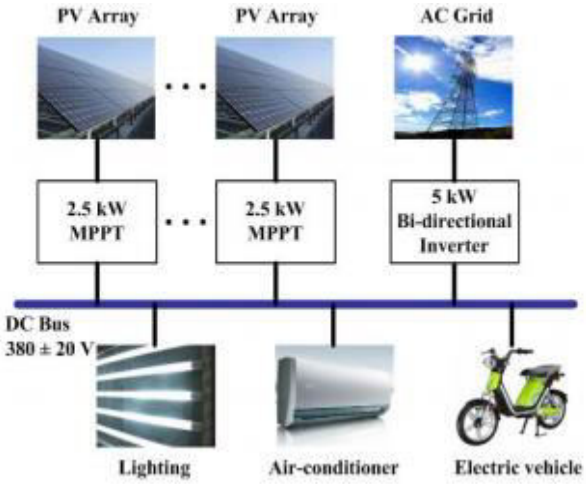

Fig.1. Configuration of a dc distribution system

II. OPERATIONAL PRINCIPLE AND CONTROL LAWS FOR THE INVERTER

To achieve the desired performance of the proposed PV inverter system, its operational principle is first presented and the control laws for the inverter operation are then derived. Fig. 3 shows a configuration of the proposed single-phase bi-directional inverter with two buck/boost MPPTs, which can fulfill either grid-connection mode or rectification mode with PFC. The proposed bi-directional inverter, is a full-bridge configuration, which can fulfill grid connection and rectification with PFC. The inverter senses dc bus voltage vdc, line voltage vs and inductor current iLs, and uses the variable inductance, which is a function of inductor current, obtained with self-learning algorithm to determine the control for operating the inverter stably. When the output power from PV arrays is higher than load requirement, the dc bus voltage increases; thus, the inverter is operated in grid-connection mode to inject the surplus power into ac grid. On the other hand, the inverter is operated in rectification mode with PFC to convert ac source to replenish the dc bus. Unlike the uni-

International Journal for Innovative Engineering and Management Research
A Peer Revieved Open Access International Journal
www.ijiemr.org

polar modulation, the dead beat control laws with a bipolar modulation are derived as follows:

$$d_{gc} = \frac{1}{2} + \frac{|v_s|}{2v_{dc}} + \frac{\Delta i_{Ls} \cdot L_s(i_{Ls})}{2v_{dc} \cdot T_s} \text{ (for grid-connection mode)} \quad (1)$$

And

$$d_{re} = \frac{1}{2} - \frac{|v_s|}{2v_{dc}} + \frac{\Delta i_{Ls} \cdot L_s(i_{Ls})}{2v_{dc} \cdot T_s}, \text{ (for rectification mode)} \quad (2)$$

Where Ts is the switching period and dgc and dre are the duty ratios (controls). A control block diagram of the inverter with bipolar modulation is shown in Fig. 4. According to the reference current difference (iref(n+1)-iref(n)) and the current error ie(n) between reference current iref(n) and feedback current ifb(n), the controller can determine duty ratio d(n+1) for the (n+1) cycle. In (1) and (2), the total current difference ΔiLs can be expressed as follows:

$$\Delta i_{Ls}(n+1) = i_{ref}(n+1) - i_{ref}(n) + K_p \cdot i_e(n) \quad (3)$$

Where

$$i_e(n) = i_{ref}(n) - i_{fb}(n) \quad (4)$$

The controller finely adjusts the duty ratio based on (1) or (2) and keeps with Kp = 1 to compensate the current error ie(n). Feedback gain H is a scaling factor when sensing inductor current iLs. According to the duty ratio shown in (1) and (2), the Gc can be determined as follows:

$$G_c = L_s(i_{Ls}) / 2v_{dc} T_s \quad (5)$$

Where Ls(iLs) is the learned inductance which varies with iLs. The plant Gp of the inverter is defined as the transfer function of control d to inductor current iLs, which can be derived based on state-space averaging method [19] as follows:

$$G_p(s) = \frac{i_{Ls}}{d} = \frac{v_{dc}}{sL_s + r_l} \quad (6)$$

Where rl is the equivalent resistance of Ls

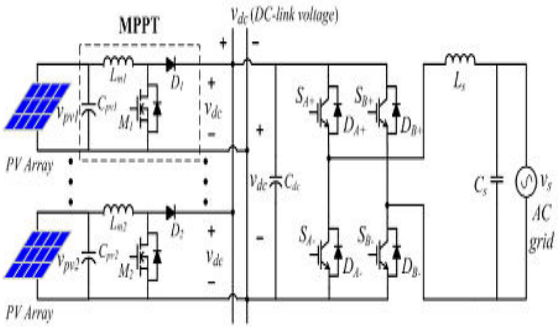

Fig.2. A conventional two stage PV inverter system with boost-type MPPTs.

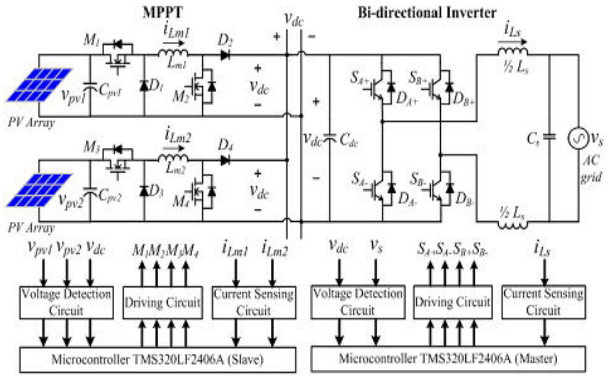

Fig.3. Configuration of the studied PV inverter system with the buck/boost MPPTs

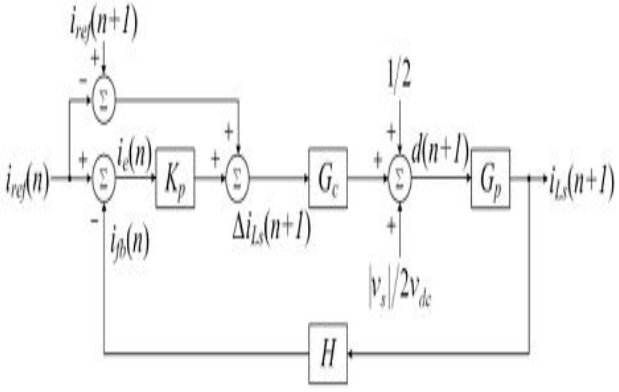

Fig.4. a control block diagram of the bi-directional inverter with bipolar modulation

Since the load may change abruptly and cause dc-bus voltage varying beyond the operating range, it requires a regulation mechanism to control the dc-bus voltage to a certain range. The bi-directional inverter will adjust the inductor current command to balance the power and regulate the dc-bus voltage.

International Journal for Innovative Engineering and Management Research
A Peer Revieved Open Access International Journal
www.ijiemr.org

III. OPERATION AND ANALYSIS OF THE PROPOSED BUCK/BOOST MPPTS

The MPPT topology is formed from a buck converter and a boost converter but with a shared inductor to accommodate wide PV-array voltages from 0 to 600 V. For various PV-array applications, the two MPPTs will be connected separately or in parallel. The MPPT senses PV voltage vpv, dc-bus voltage vdc and inductor current iLm into the single-chip microcontroller (TMS320LF2406A) to determine operational mode and duty ratio for tracking the maximum power point accurately. When voltage vpv is higher than vdc, the MPPT is operated in buck mode, and switch M1 is turned on to magnetize inductor Lm and thus increase inductor current iLm. While switch M1 is turned off, inductor Lm releases its stored energy through diodes D1 and D2. On the other hand, the MPPT is operated in boost mode when voltage vpv is lower than vdc, and switches M1 and M2 are turned on to magnetize inductor Lm. While switch M2 is turned off, inductor Lm releases its stored energy through diode D2. Thus, the control laws can be expressed as follows:

$$d_{buck} = \frac{v_{dc}}{v_{pv}} \text{ (for buck mode)} \quad (7)$$

And

$$d_{boost} = \frac{v_{dc} - v_{pv}}{v_{dc}} \text{. (for boost mode)} \quad (8)$$

To draw maximum power from PV arrays, a perturbation and observation control algorithm for tracking maximum power points is adopted. If the maximum power level of a PV array is higher than the power rating of an MPPT, the two MPPTs will be in parallel operation to function as a single MPPT. Thus, it requires an on-line configuration check to determine the connection types of the two MPPTs, separate or in parallel. Moreover, if the two MPPTs are in parallel operation, a uniform current control scheme is introduced to equally distribute the PV-array output current to the two MPPTs. The operational mode transition control between buck and boost is also presented.

A. Perturbation and Observation Tracking Method

In this study, the MPPT controller tracks the maximum output power of a PV array based on the perturbation and observation tracking method. At the beginning, the controller will determine the operation mode of the proposed MPPT. When the MPPT is operated in boost mode, inductor current iLm is equal to output current ipv of the PV array; thus, the output power of the PV array can be expressed as follows:

$$P_{pv\_boost}(n) = v_{pv}(n) \times i_{Lm}(n) \quad (9)$$

On the other hand, when the proposed MPPT is operated in buck mode, inductor current iLm is equal to output current io; thus, the output power of the PV array can be expressed as follows:

$$P_{pv\_buck}(n) = v_{dc}(n) \times i_{Lm}(n) \quad (10)$$

With this control algorithm, the controller tracks the peak power by increasing or decreasing the duty ratio periodically. In this studied PV inverter system, there is a shared auxiliary power supply for the MPPTs and the inverter. Because the switching frequencies of the MPPT (25 kHz) and the inverter (20 kHz) are different, their switching noises might affect the accuracy of voltage and current sampling, especially under high power condition. To avoid noise interference, the MPPTs are synchronized with the inverter, and the controller will update the duty ratio of the MPPT power stage every 10 line cycles at the zero crossing of the line voltage. Additionally, since the single-phase PV inverter system has a twice line-frequency ripple voltage on the dc bus, this synchronization approach can also eliminate the ripple voltage effect and

International Journal for Innovative Engineering and Management Research
A Peer Revieved Open Access International Journal
www.ijiemr.org

determine accurate output power of the PV arrays. When the output power of the PV arrays can be determined accurately, the proposed controller can track the maximum power point precisely.

B. On-Line MPPT Configuration Check

In order to track the maximum power point correctly and effectively, a scheme of on-line MPPT configuration check is proposed. A flowchart of the check algorithm is shown in Fig.5. First, the MPPT determines if there is any PV array plugged in or removed from the system by checking voltage vpv for 100 ms. If voltage vpv is higher than threshold voltage vth, the controller determines that a new PV array is plugged into an MPPT. On the contrary, if voltage vpv is lower than vth, it means that a PV array is removed from an MPPT, or there is no PV array. Next, if the input voltages of both MPPTs are very close (within Δv), the MPPT configuration will be determined as a parallel mode. On the contrary, the two MPPTs will be operated in separate mode. Moreover, a parallel verification algorithm is utilized to confirm the MPPT configuration check. The controller will perturb the duty ratio of one MPPT to examine if both MPPT input voltages are still identical to indentify the connection modes.

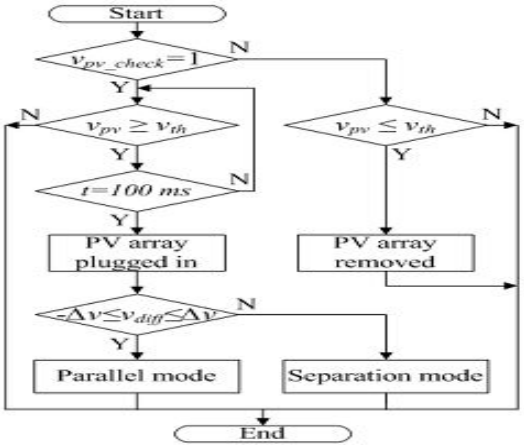

Fig.5. Flowchart of on-line MPPT configuration check

The system controller checks the configuration of the MPPTs every switching cycle. If the PV arrays are connected to the MPPTs separately, as shown in Fig. 4(a), the MPPTs will calculate their PV output power and tune their duty ratios individually. If the maximum power level of a PV array is higher than that of an MPPT, the two MPPTs will be connected to this PV array and operated synchronously, as shown in Fig. 4(b). When tracking the maximum PV output power, the MPPTs will sum up their input currents and equally distribute the total current to the two MPPTs based on a uniform current control scheme.

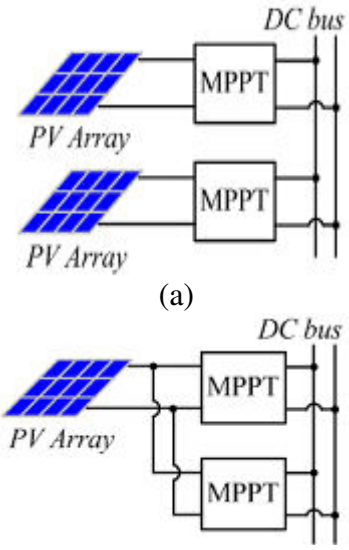

Fig.6. Input configuration of the two MPPTs: (a) separate, and (b) in parallel

C. Uniform Current Control Scheme

There might exist differences between the two MPPTs, such as components, feedback signals and noise levels, which will result in current imbalance while they are connected in parallel. When a current imbalance occurs, the components with higher current level will suffer from higher temperature and shorter life time. Considering the component reliability and thermal problem, a uniform current

International Journal for Innovative Engineering and Management Research
A Peer Revieved Open Access International Journal
www.ijiemr.org

control scheme is proposed and described as follows. First, we calculate the current difference (Δidiff) between the two MPPTs to determine if a uniform current control is necessary. If the current difference Δidiff is higher than a threshold value, the controller will vary the duty ratios (Δd) of the MPPTs to achieve equal current distribution. The duty ratios of the two MPPTs are determined as follows:

$$D_{pv1} \leftarrow D_{pv1} \pm \Delta d \quad (11)$$

And

$$D_{pv2} \leftarrow D_{pv2} \mp \Delta d \quad (12)$$

In which when Dpv1 is increased by Δd and Dpv2 will be decreased by Δd, and vice versa.

D. Buck-Boost Mode Transition

Since the operation range of the dc-bus voltage is limited within 380±20V (including ripple voltage) in the dc distribution system, operational mode transition between the buck and boost modes will be a critical control issue to accommodate a wide PV input voltage variation (0 to 600 V).

When the proposed MPPT is operated in boost mode and voltage vpv is close to vdc, switch M2 is turned off and the duty ratio of switch M1starts to decrease (-Δd) from 100 %. With this control scheme, current ipv of the PV array will charge input capacitor Cpv, and voltage vpv can be raised up to a higher level to prevent mode fluctuation problems. On the contrary, switch M1 is continuously turned on and the duty ratio of switch M2 starts to increase (+Δd) from 0 %, when vpv drops towards vdc during buck mode.

Therefore, the MPPT can achieve smooth mode transition by tuning the duty ratios of the active switches. A flowchart of the buck/boost mode transition scheme is shown in Fig. 7.

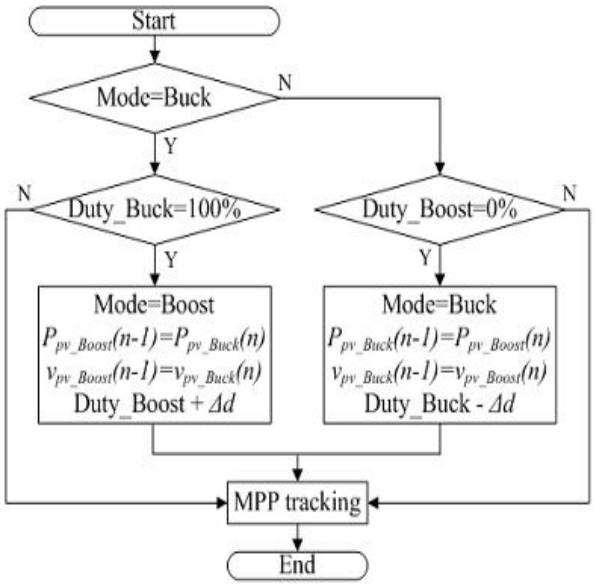

Fig.7. Flowchart of the buck/boost mode transition algorithm

IV. DC-BUS VOLTAGE REGULATION MECHANISM

The proposed regulation mechanism is similar to the concept of the AVP method [20], but it is more like a droop one. In the discussed dc-distribution system, for reducing dc-bus capacitance and mode-change frequency, a droop dc-bus voltage regulation mechanism is proposed, as illustrated in Fig. 8, in which the dc-bus voltage is regulated according to the inductor current linearly. When the bi-directional inverter sells higher power, which means less load power requirement, the dc-bus voltage will be regulated to a higher level. If there is a heavy step load change suddenly, this mechanism can avoid a voltage drop below 380 V abruptly and it will not change the operation mode from grid connection to rectification, or can avoid under voltage protection. On the other hand, when the bi-directional inverter buys higher power, the dc-bus voltage is regulated to a lower level, reducing the frequency of mode change and thus reducing the dc-bus capacitance around 15 %.

International Journal for Innovative Engineering and Management Research
A Peer Revieved Open Access International Journal
www.ijiemr.org

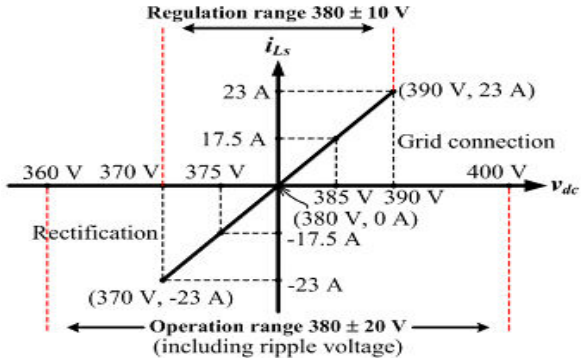

Fig.8. Illustration of a dc-bus voltage regulation mechanism with a linear relationship between inductor current iLs and dc-bus voltage vdc.

$$\Delta i_{dc} = C_{dc} \frac{v_{dc}(n) - v_{dc}(n-1)}{t_n - t_{x1}} \quad (13)$$

From the linear dc-bus voltage regulation relationship shown in Fig. 8, the new steady state voltage vdc can be obtained. Therefore, the adjustment current command IA can be determined. The control laws can adjust inductor-current command and regulate the dc-bus voltage to its corresponding level simultaneously. Since time tx1is unpredictable, we approximate the time difference (Δt = tn-tx1) with one line cycle Tl, and new inductor-current command IA(n) can be determined based on previous current command IA(n-1) as follows:

$$I_A(n) = I_A(n-1) + f_l C_{dc}\left(v_{dc}(n) - v_{dc}(n-1)\right) + f_l C_{dc}\left(v_{dc}(n) - v_{dc}(n+1)\right) \quad (14)$$

Where fl is the line frequency and voltage vdc (n+ 1) can be derived as follows based on the linear relationship shown in Fig. 8.

$$v_{dc}(n+1) = 380\,V + \frac{10\,V}{23\,A} I_A(n+1) \cdot \frac{\left(v_{dc}(n) + v_{dc}(n+1)\right)}{220 \times 2} \quad (15)$$

Where

$$I_A(n+1) = I_A(n-1) + \Delta I \quad (16)$$

And

$$\Delta I = C_{dc} \frac{v_{dc}(n) - v_{dc}(n-1)}{T_l} = f_l C_{dc}\left(v_{dc}(n) - v_{dc}(n-1)\right) \quad (17)$$

V. CUK CONVERTER

The Cuk converter is a type of DC/DC converter that has an output voltage magnitude that is either greater than or less than the input voltage magnitude. It is essentially a boost converter followed by a buck converter with a capacitor to couple the energy. Similar to the buck–boost converter with inverting topology, the output voltage of non-isolated Cuk is typically also inverting, and can be lower or higher than the input. It uses a capacitor as its main energy-storage component, unlike most other types of converters which use an inductor.

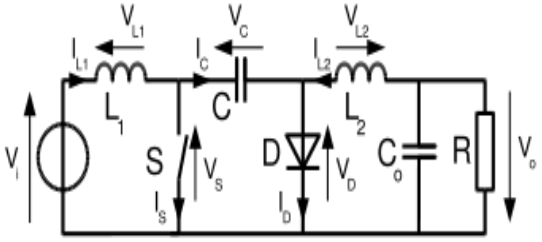

Fig.9 Schematic of a Cuk converter.

A Cuk converter comprises two inductors, two capacitors, a switch (usually a transistor), and a diode. Its schematic can be seen in figure 9. It is an inverting converter, so the output voltage is negative with respect to the input voltage.

The capacitor C is used to transfer energy and is connected alternately to the input and to the output of the converter via the commutation of the transistor and the diode (sees figures 10).

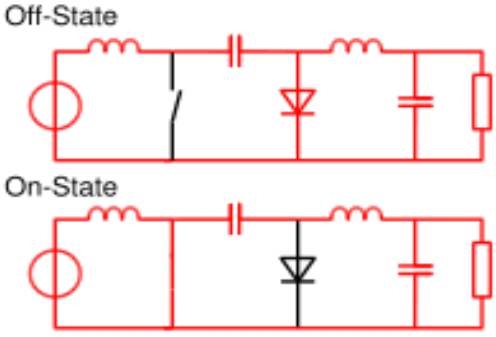

Fig.10 The two operating states of a Cuk converter.

International Journal for Innovative Engineering and Management Research
A Peer Revieved Open Access International Journal
www.ijiemr.org

VI. MATLAB/SIMULINK RESULTS

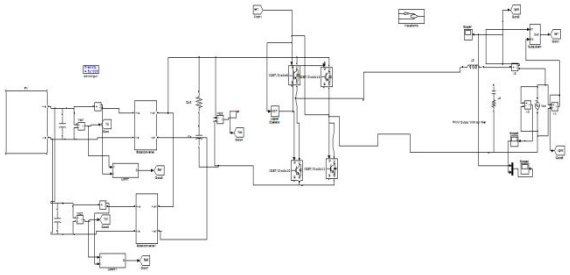

Fig.11 MATLAB/SIMULINK circuit of PV inverter system with the buck/boost MPPTs

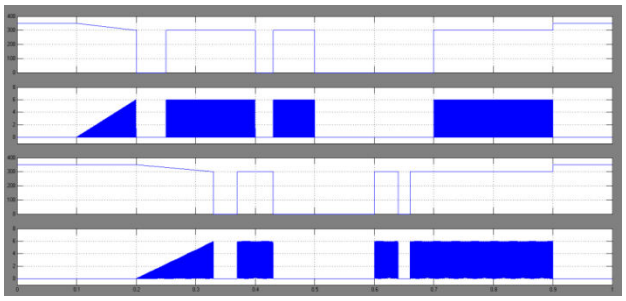

Fig.12 Output waveform of PV voltages and inductor current in separate condition

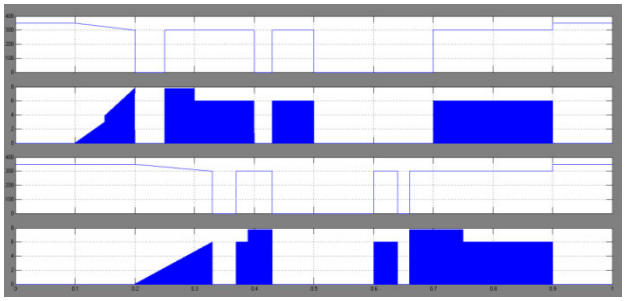

Fig.13 Output waveform of PV voltages and inductor currents in parallel condition

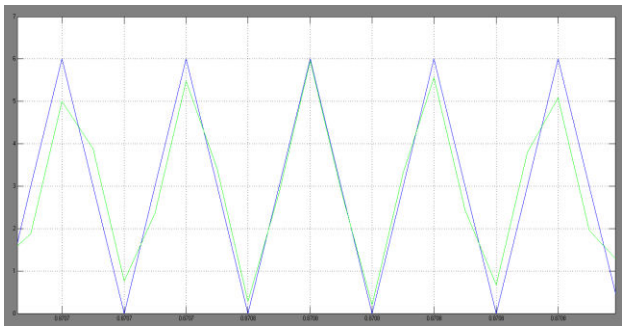

Fig.14 Output waveform of difference between inductor currents

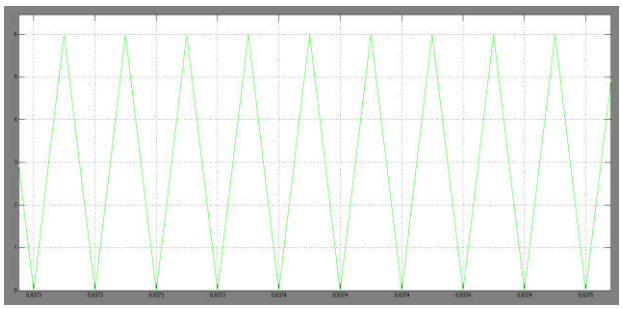

Fig.15 Output waveform of uniform current distribution of inductor currents

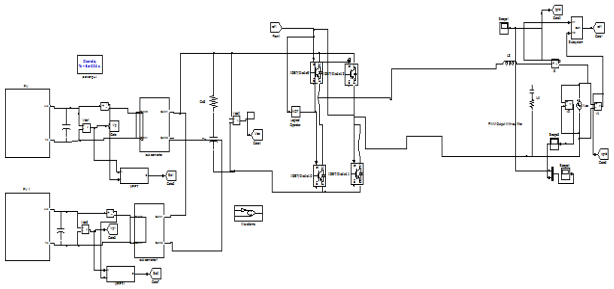

Fig.16 MATLAB/SIMULINK circuit of PV inverter system with Cuk converter MPPTs

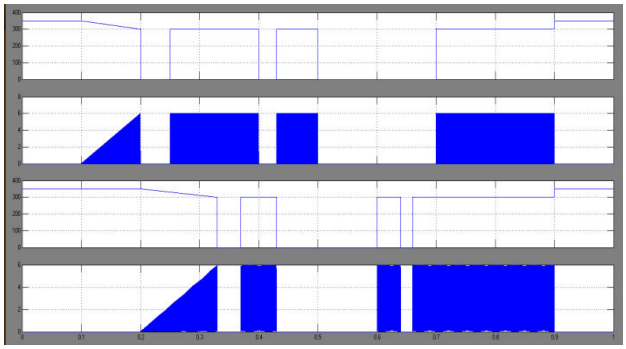

Fig.17 Cuk converter PV voltages and inductor currents output waveforms

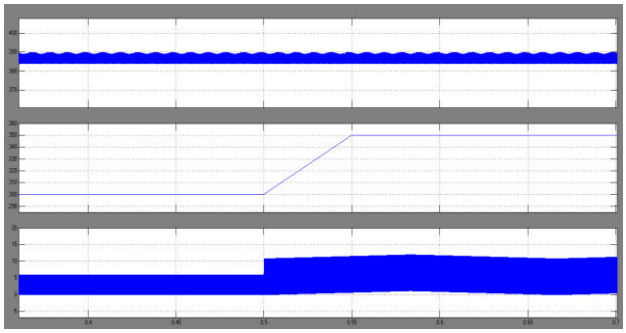

Fig.18 Output waveform of DC-link voltage PV voltage and Inductor current voltage in Boost to Buck mode condition

International Journal for Innovative Engineering and Management Research
A Peer Revieved Open Access International Journal
www.ijiemr.org

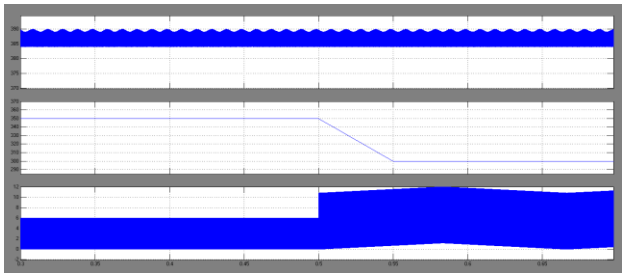

Fig.19 Output waveform of DC-link voltage PV voltage and Inductor current voltage in Buck to Boost mode condition

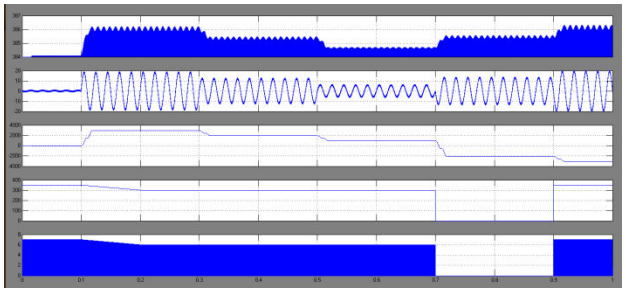

Fig.20 Dc-link voltage, Inductor currents iLm, iLs, Active PV voltage, Active and Reactive power

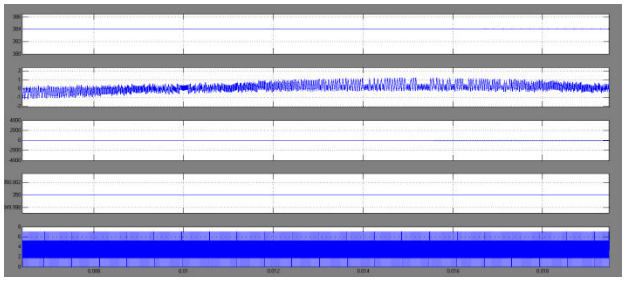

Fig.21 Measured waveforms of PV output voltage vpv, dc-bus voltage vdc, inductor current iLm1 and iLs during MPPTs soft start.

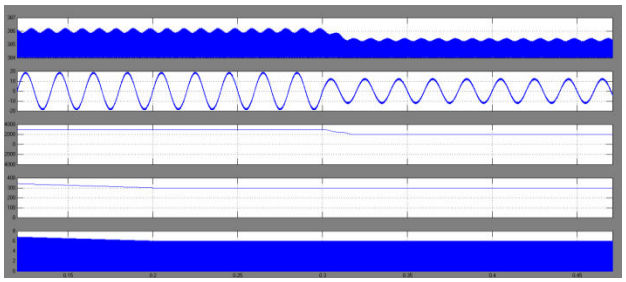

Fig.22 Measured waveforms of PV output voltage vpv, dc-bus voltage vdc, inductor currents iLm1 and iLs when the dc load varying from no load to 1 kW

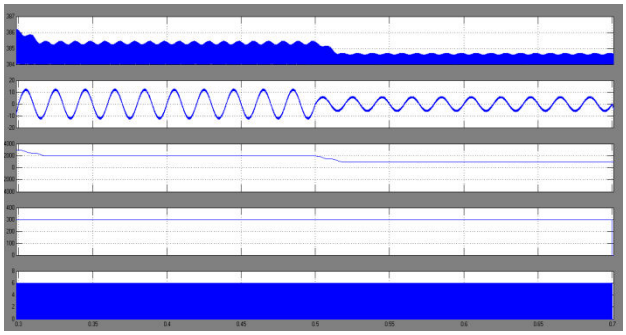

Fig.23 Measured waveforms of PV output voltage vpv, dc-bus voltage vdc, inductor currents iLm1 and iLs when the dc load varying from 1 kW to 2 kW under 3 kW PV output power.

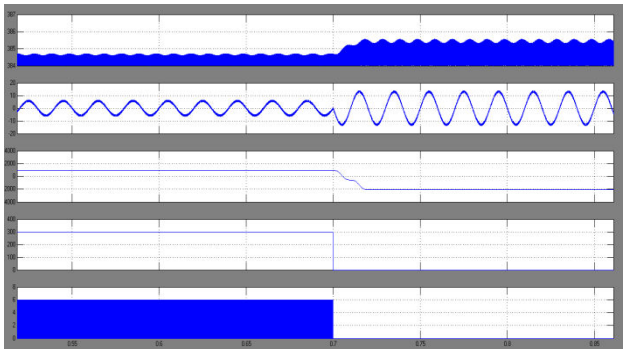

Fig.24 Measured waveforms of PV output voltage vpv, dc-bus voltage vdc, inductor currents iLm1 and iLs when operational mode changing from grid connection to rectification at MPPT shutdown.

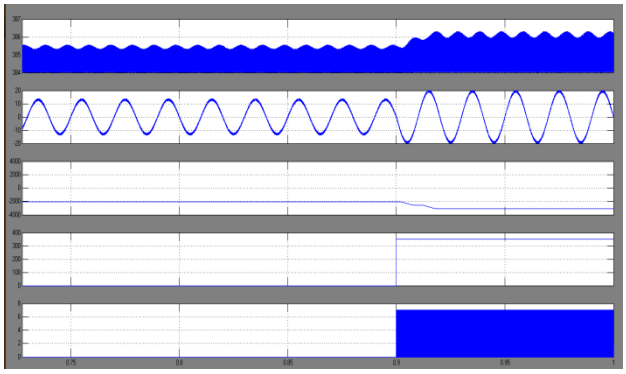

Fig.25 Measured waveforms of PV output voltage vpv, dc-bus voltage vdc, inductor currents iLm1 and iLs when the dc load varying from 2 kW to 3 kW during MPPTs shutdown.

International Journal for Innovative Engineering and Management Research
A Peer Revieved Open Access International Journal
www.ijiemr.org

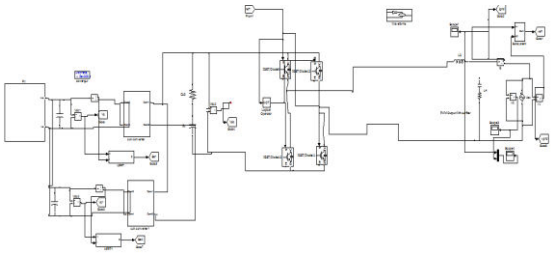

Fig.26 MATLAB/SIMULINK circuit of PV inverter system with Cuk converter MPPTs

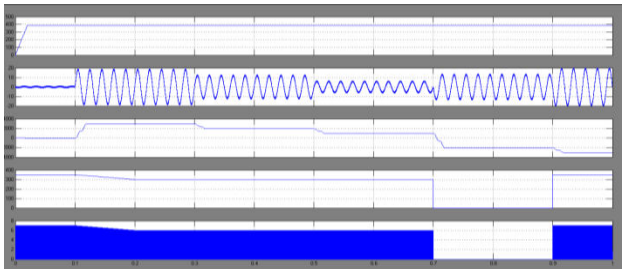

Fig.27 Dc-link voltage, Inductor currents iLm, iLs, Active PV voltage, Active and Reactive power

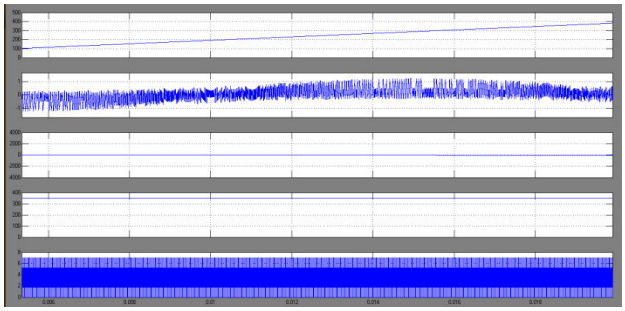

Fig.28 Measured waveforms of PV output voltage vpv, dc-bus voltage vdc, inductor current iLm1 and iLs during MPPTs soft start.

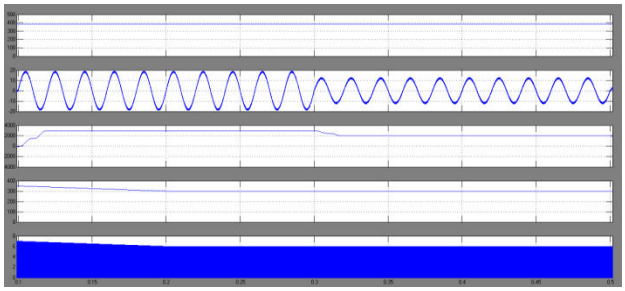

Fig.29 Measured waveforms of PV output voltage vpv, dc-bus voltage vdc, inductor currents iLm1 and iLs when the dc load varying from no load to 1 kW

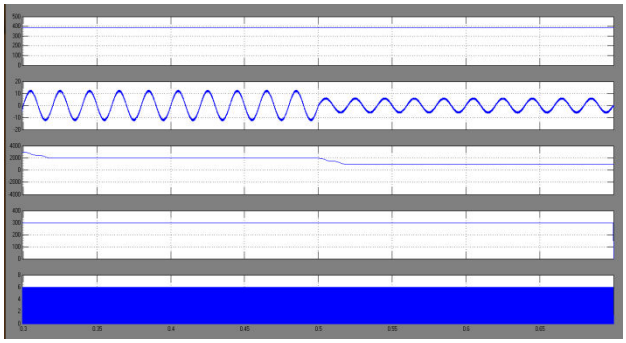

Fig.30 Measured waveforms of PV output voltage vpv, dc-bus voltage vdc, inductor currents iLm1 and iLs when the dc load varying from 1 kW to 2 kW under 3 kW PV output power.

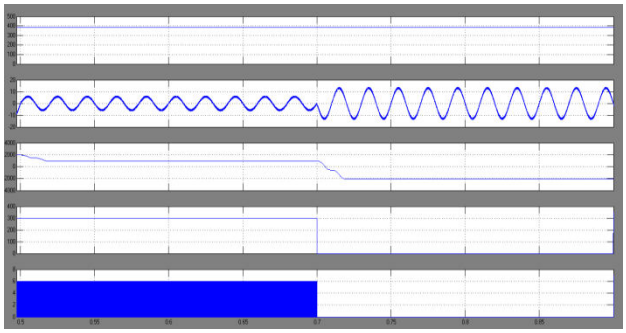

Fig.31 Measured waveforms of PV output voltage vpv, dc-bus voltage vdc, inductor currents iLm1 and iLs when operational mode changing from grid connection to rectification at MPPT shutdown.

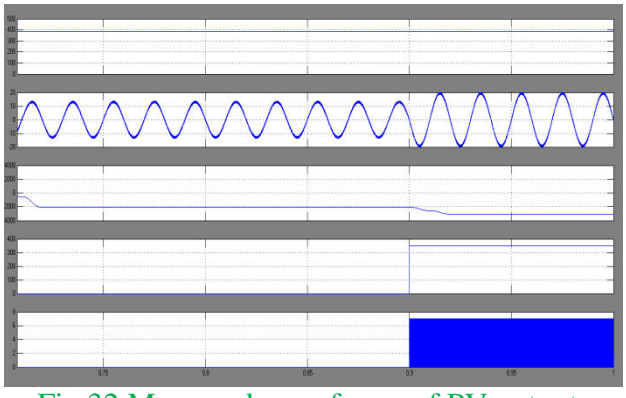

Fig.32 Measured waveforms of PV output voltage vpv, dc-bus voltage vdc, inductor currents iLm1 and iLs when the dc load varying from 2 kW to 3 kW during MPPTs shutdown.

VII. CONCLUSION

This paper deals with the integrated operation of two Cuk converters and a single phase bidirectional inverter. The Cuk converter is a DC-DC converter in which the output voltage may be greater than, lesser than or equal to that of input voltage. The DC voltage is converted into AC voltage by means of a single phase bidirectional inverter. During the grid connection operation, the bidirectional inverter will convert the DC into AC voltages by using PWM signals. During the rectification operation the inverter act as converter and convert the AC voltage into DC voltage. The maximum power point tracking algorithm used is hill climbing method, which deals with perturbing the duty cycle and maximum power is obtained. The operation of DC loads are quiet easier than an AC loads, since the integration of AC loads requires frequency matching AC-AC converters along with grid synchronization, power factor problems, grid stability issues and so on. Hence in future work rectification of these operating problems and a reliable grid connected solar operation should be done.

REFERENCES

[1] J. M. Carrasco, L. G. Franquelo, J. T. Bialasiewicz, E. Galvan, R. C. P. Guisado, Ma. A. M. Prats, J. I. Leon, and N. Moreno-Alfonso, "Power-electronic systems for the grid integration of renewable energy sources: a survey," IEEE Trans. on Ind. Electron., vol. 53, no. 4, pp. 1002-1016, Aug. 2006.

[2] L. N. Khanh, J.-J. Seo, T.-S. Kim, and D.-J. Won, "Power-management strategies for a grid-connected PV-FC hybrid system," IEEE Trans. on Power Deliv., vol. 25, no. 3, pp. 1874-1882, Jul. 2010.

[3] Y. K. Tan and S. K. Panda, "Optimized wind energy harvesting system using resistance emulator and active rectifier for wireless sensor nodes," IEEE Trans. on Power Electron., vol. 26, no. 1, pp. 38-50, Jan. 2011.

[4] J.-M. Kwon, K.-H. Nam, and B.-H. Kwon, "Photovoltaic power conditioning system with line connection," IEEE Trans. on Ind. Electron., vol. 53, no. 4, pp. 1048-1054, Aug. 2006.

[5] J. Selvaraj and N. A. Rahim, "Multilevel inverter for grid-connected PV system employing digital PI controller," IEEE Trans. on Ind. Electron., vol. 56, no. 1, pp. 149-158, Jan. 2009.

[6] F. Gao, D. Li, P. C. Loh, Y. Tang, and P. Wang, "Indirect dc-link voltage control of two-stage single-phase PV inverter," Proceedings of the 2009 IEEE ECCE, pp. 1166-1172, 2009.

[7] A. Nami, F. Zare, A. Ghosh, and F. Blaabjerg, "A hybrid cascade converter topology with series-connected symmetrical and asymmetrical diode-clamped H-Bridge cells," IEEE Trans. on Power Electron., vol. 26, no. 1, pp. 51-65, Jan. 2011.

[8] S. Dwari and L. Parsa, "An efficient high-step-up interleaved dc–dc converter with a common active clamp," IEEE Trans. on Power Electron., vol. 26, no. 1, pp. 66-78, Jan. 2011.

[9] J.-M. Shen, H.-L. Jou, and J.-C. Wu, "Novel transformerless grid connected power converter with negative grounding for photovoltaic generation system," IEEE Trans. on Power Electron., vol. 27, no. 4, pp. 1818-1829, Apr. 2012.

[10] T. Kerekes, R. Teodorescu, P. Rodriguez, G. Vazquez, and E. Aldabas, "A new high-efficiency single-phase transformerless PV

inverter topology," IEEE Trans. on Ind. Electron., vol. 58, no. 1, pp. 184-191, Jan. 2011.

[11] S. V. Araujo, P. Zacharias, and R. Mallwitz, "Highly efficient single-phase transformerless inverters for grid-connected photovoltaic systems," IEEE Trans. on Ind. Electron., vol. 57, no. 9, pp. 3118-3128, Sep. 2010.

[12] J. S. Park, J. H. Choi, B. G. Gu, I. S. Jung, E. C. Lee, and K. S. Ahn, "Robust dc-link voltage control scheme for photovoltaic power generation system PCS," Proceedings of the 31st International on Telecommunications Energy Conference, pp. 1-4, 2009.

[13] D. Salomonsson, L. Soder and A. Sannino, "An adaptive control system for a dc microgrid for data centers," IEEE Trans. on Ind. Appl., vol. 44, no. 6, pp. 1910-1917, Nov. 2008.

[14] M. A. Azzouz and A. L. Elshafei, "An adaptive fuzzy regulation of the dc-bus voltage in wind energy conversion systems," Proceedings of the 2010 IEEE International Conference on CCA, pp. 1193-1198, 2010.

[15] H. Kakigano, A. Nishino, Y. Miura, and T. Ise, "Distribution voltage control for dc microgrid by converters of energy storages considering the stored energy," Proceedings of the 2010 IEEE ECCE, pp. 2851-2856, 2010.